J. Kor. Powd. Met. Inst., Vol. 20, No. 4, 2013
DOI: 10.4150/KPMI.2013.20.4.275

An Investigation of the Stability of Y_2O_3 and Sintering Behavior of Fe-Based ODS Particles Prepared by High Energy Ball Milling

Eun-Kwang Park[a,b], Sung-Mo Hong[b,c], Jin-Ju Park[b,*], Min-Ku Lee[b], Chang-Kyu Rhee[b] and Kyeong-won Seol[a]

[a]*Department of Metallurgical Engineering, Jeonbuk National University, Jeonju 330-717, Korea*
[b]*Nuclear Materials Development Division, Korea Atomic Energy Research Institute (KAERI), Daejeon 305-353, Korea*
[c]*Division of Advanced Materials Engineering, Kongju National University, Cheonan 330-717, Korea*
(Received August 12, 2013; Accepted August 23, 2013)

Abstract Fe-based oxide dispersion strengthened (ODS) powders were produced by high energy ball milling, followed by spark plasma sintering (SPS) for consolidation. The mixed powders of 84Fe-14Cr-2Y_2O_3 (wt%) were mechanically milled for 10 and 90 mins, and then consolidated at different temperatures (900~1100ºC). Mechanically-Alloyed (MAed) particles were examined by means of cross-sectional images using scanning electron microscopy (SEM). Both mechanical alloying and sintering behavior was investigated by X-ray diffraction (XRD) and high resolution transmission electron microscopy (HR-TEM). To confirm the thermal behavior of Y_2O_3, a replica method was applied after the SPS process. From the SEM observation, MAed powders milled for 10 min showed a lamella structure consisting of rich regions of Fe and Cr, while both regions were fully alloyed after 90 min. The results of sintering behavior clearly indicate that as the SPS temperature increased, micro-sized defects decreased and the density of consolidated ODS alloys increased. TEM images revealed that precipitates smaller than 50 nm consisted of $YCrO_3$.

Keywords : Oxide dispersion strengthened (ODS) alloy, Yttria, High energy ball milling, Spark plasma sintering (SPS), Sintering behavior

1. Introduction

Mechanically-alloyed oxide dispersion strengthened (MA ODS) alloys exhibit high strength and an outstanding creep property owing to the existence of fine grains and dispersed fine oxide particles. To obtain this specific property, pre-alloyed metal and Y_2O_3 powders are usually ball milled, and then thermo-mechanical treatments are applied [1]. Yttria (Y_2O_3) is widely utilized as an oxide for reinforcement, because it has thermo-dynamical and chemical stability. For that reason, ODS alloys are promising materials for nuclear applications. Among them, ferritic alloys prossess more radiation resistant than austenitic alloys due to the ferritic microstructure at elevated temperature around 973K [2-4], and therefore, many previous experiments have been focused on modifying chemical compositions and preparation methods for finely dispersed oxide particles [5-7]. In order to produce ODS alloys, MA was involved in the synthesis of materials. Complete synthesis of Y_2O_3 in matrix powders during MA is essential for a homogeneous dispersion of oxide particles. In recent years, a throughful study on phase change of Y_2O_3 during MA has been reported. However, we still have to clarify mechanism about formation behavior of Y_2O_3 from MA to consolidation.

In this work, to confirm clearly the behavior of Y_2O_3, simplified Fe-14Cr-2Y_2O_3 ODS ferritic alloy was produced by a mechanical alloying (MA) and spark plasma sintering (SPS) method for an investigation into the stability of Y_2O_3 and sintering behavior of Y_2O_3 particles during the MA and SPS process.

*Corresponding Author : Jin-Ju Park, **TEL:** +82-42-868-4834, **FAX:** +82-42-868-8275, **E-mail:** jinjupark@kaeri.re.kr

2 Experimental Procedure

The chemical composition of the starting particles used in this work was 84Fe-14Cr-2Y_2O_3 (wt%). All of them were more than 99.9% pure, and their average size was from 40 to 50 μm. The mechanical alloying of Fe(E04PB, HPC), Cr(E08PB, HPC) and Y_2O_3(LTS Inc.) particles was performed by a specially designed high energy ball mill machine (TMC P300)[8] under an Ar (high purity) atmosphere for various milling times of 10 and 90 mins. The bowl which contained a Fe based powder mixture (10 g) and the stainless steel balls 8 mm in diameter (200 g) were rotated at a speed of 850 rpm and the weight ratio of the balls to the powders was set at 20:1. After mechanical alloying, the two types of powders milled for 10 and 90 min were consolidated by means of spark plasma sintering at 900, 1000, and 1100°C for 30 min. The SPS holding times were fixed in all conditions.

The MAed powders and sintered ODS alloys were analyzed by X-ray diffraction (XRD, Rigaku D/MAX 2500H) using Cu Kα radiation operating at 40 kV and 100 mA. To confirm the behavior of mechanical alloying, the cross section of Fe based powders was characterized using scanning electron microscopy (SEM, FEI Sirion). The sintering behavior was analyzed by optical microscope (OM, Olympus), and the relative density was calculated by means of the Archimedes method. The observation of the oxide particles was performed using high resolution transmission electron microscopy (HR-TEM, JEOL JEM-2100F) with EDS. The TEM samples were prepared using the conventional electro-polishing method and a replica method [3,9-10]. Extraction replicas can give us more coherent information about oxide analysis without a matrix.

3. Results and Discussion

3.1. Mechanical alloying behavior

Generally, ball milling has an effect on the pre-alloying, size reduction, and uniform distribution of powder materials. In the present work, it was adopted as the first means of finely dispersing oxide particles in sintered alloys. The resulting cross-sectional images of MAed ODS powders prepared for 10 and 90 min are presented in Fig. 1. in the case of the MAed powder for 10 min (MA10), a lamellar structure consisted of a bright Fe rich region and a relatively dark Cr rich one was observed. Two metals were stacked in the form of layer-by-layer because the mechanical alloying was not yet finished. On the other hand, in case of MAed powder for 90 min (MA90), it was hard to distinguish one region from the other and to find Y_2O_3 particles in the matrix. In the preliminary results using our high energy ball mill machine [11], Fe-based powders were fully homogenized and the value of the lattice parameter of Fe was saturated after milling for 40 min. Eventually, compared to previous experiments [12-14], the high energy ball milling method was able to significantly reduce the MA times.

3.2. Sintering behavior

As a part of the investigation of the sintering behavior, optical images were taken to identify the characteristics of the consolidated ODS alloys using the SPS method with various temperatures, as shown in Fig. 2. in the case of a sintering temperature of 900, many defects and pores were observed, while they decreased with increasing tem-

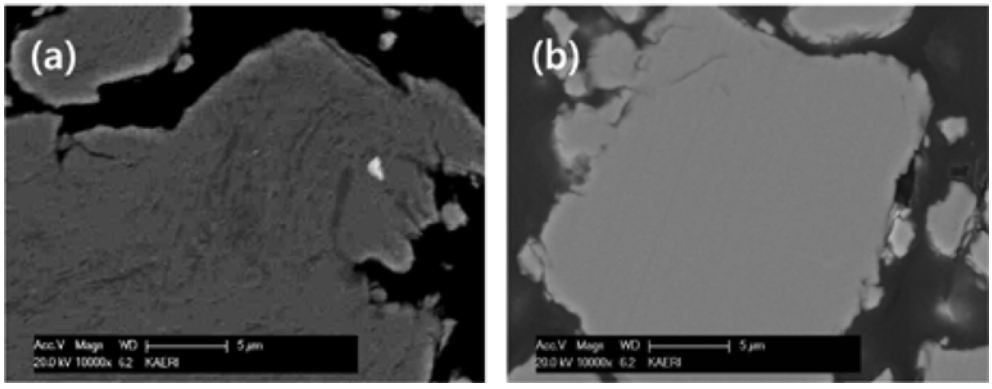

Fig. 1. SEM images of Fe-based powders with different mechanical milling times: (a) 10 min, and (b) 90 min.

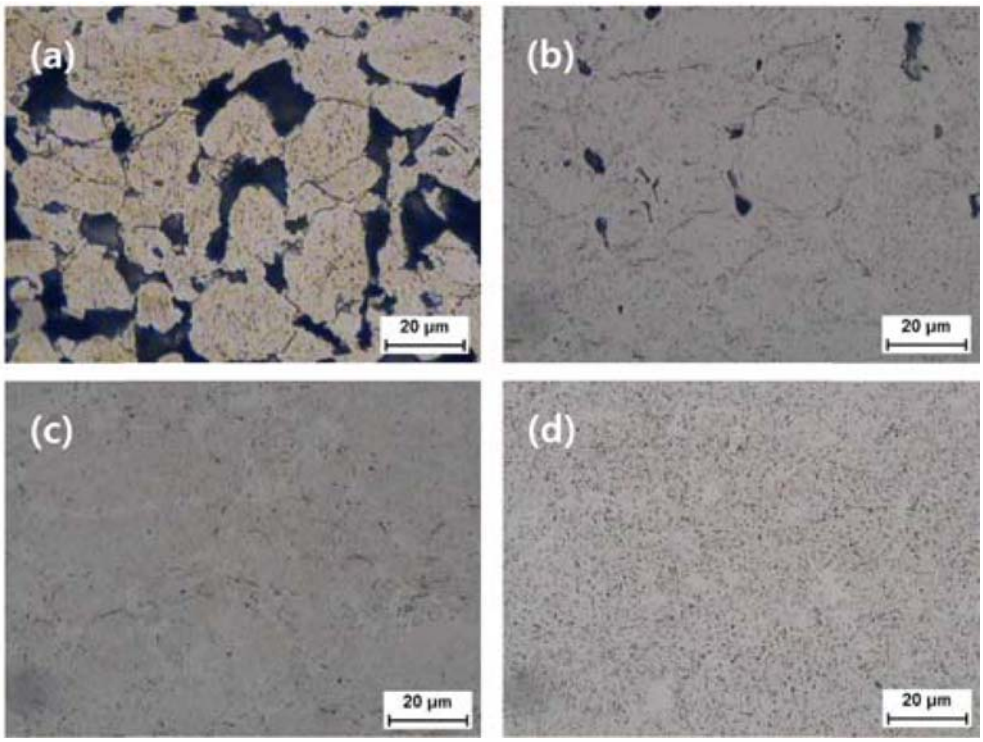

Fig. 2. OM images of ODS alloys with various consolidation temperatures at (a) 900°C (MA90), (b) 1000°C (MA90), (c) 1100°C (MA90), and (d) 1100°C (MA10).

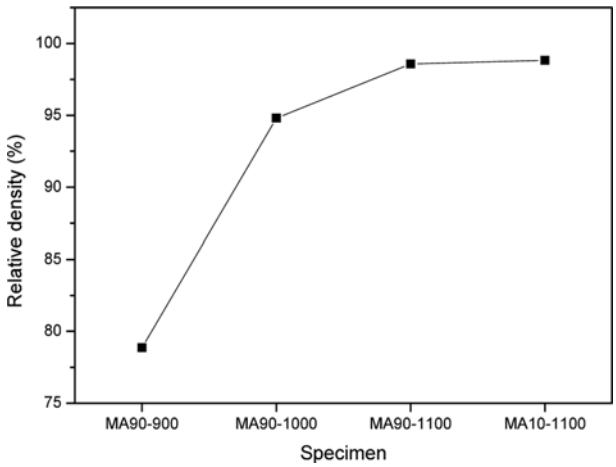

Fig. 3. Relative density of ODS alloys with various MA and SPS conditions.

perature. Micro-sized defects did not appear in the sintered specimen at 1100°C, and perfect structures were obtained. The results of the calculated relative density of sintered specimens, as shown in Fig. 3, corroborated the above OM image analysis. The initial relative density was less than 80%. As the sintering temperature rose, the value of relative density increased dramatically. However, MA time had no significant influence on the relative density. The final relative density after sintering at 1100°C was similar to the theoretical density. As a result, it was found that the SPS temperature for dense bulk must be set to more than 1100°C within the fixed holding time of 30 min.

3.3. Phase transition of Y_2O_3

The XRD results of all the MAed powders (red and black lines in Fig. 4.) revealed that the Y_2O_3 peaks were no longer detected. It was reported that, with increasing mechanical alloying time, the magnitude of these peaks decreases and their width increases due to a reduction in the crystallite size as well as an increase in the deformation amount of the particles [15]. After SPS treatment (blue and green lines in Fig. 4), many uncertain peaks and $YCrO_3$ peaks with orthorhombic structure appeared. From the different XRD patterns between MAed powders and consolidated alloys, it can be deduced that Y_2O_3 particles probably decomposed during the MA process and then reformed into $YCrO_3$ through the SPS process. For more detailed confirmation about the $YCrO_3$ phase, the results of the TEM analysis were illustrated in Fig. 5. In the first TEM image of Fig. 5(a) prepared using the

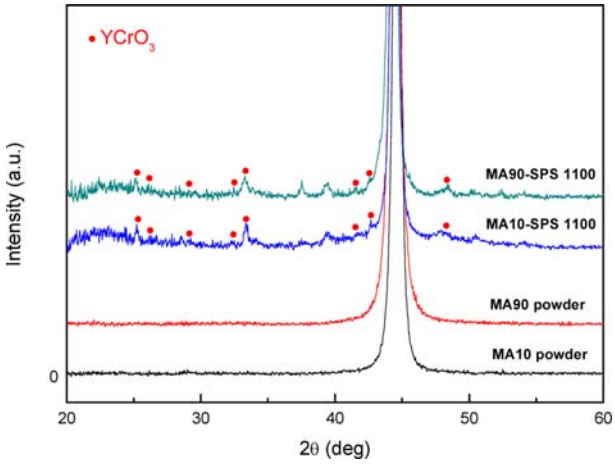

Fig. 4. XRD patterns of MAed powders and ODS alloys after SPS with various conditions.

electro-polishing method, a number of oxide precipitates were observed. Their size was measured to be smaller than 50 nm. The second TEM image of the consolidated specimen by SPS, as shown in Fig. 5(b), was prepared using the replica method. The spherical oxide precipitate has been identified as $YCrO_3$ with orthorhombic structure. This result was consistent with the XRD one. On the other hand, a consolidated specimen from MA10, similar to a lamellar layer of the previous MA process, specifically long arranged coarse oxide clusters (< 20 μm), which consist of Y-Cr-O, were presented in Fig. 5(c), and these should be treated as a defect.

4. Conclusions

The aims of the present work are to figure out the effect of various MA times and SPS temperatures on the stability of Y_2O_3 and the sintering behavior. From the experimental results, it is concluded that the MA time did not affect the sintering behavior of Fe-based ODS alloys, only SPS temperature did. On the other hand, oxide behavior was strongly influenced by the MA time. Fine and homogeneous distribution of the oxide could be made by conditions of complete mechanical alloying. The optimised condition for the production of sound Fe-based ODS alloys in this work was the SPS temperature at 1100°C and the MA time for 90 min.

Acknowledgements

This research was financially supported by the Korea Atomic Energy Research Institute (KAERI) R&D Program.

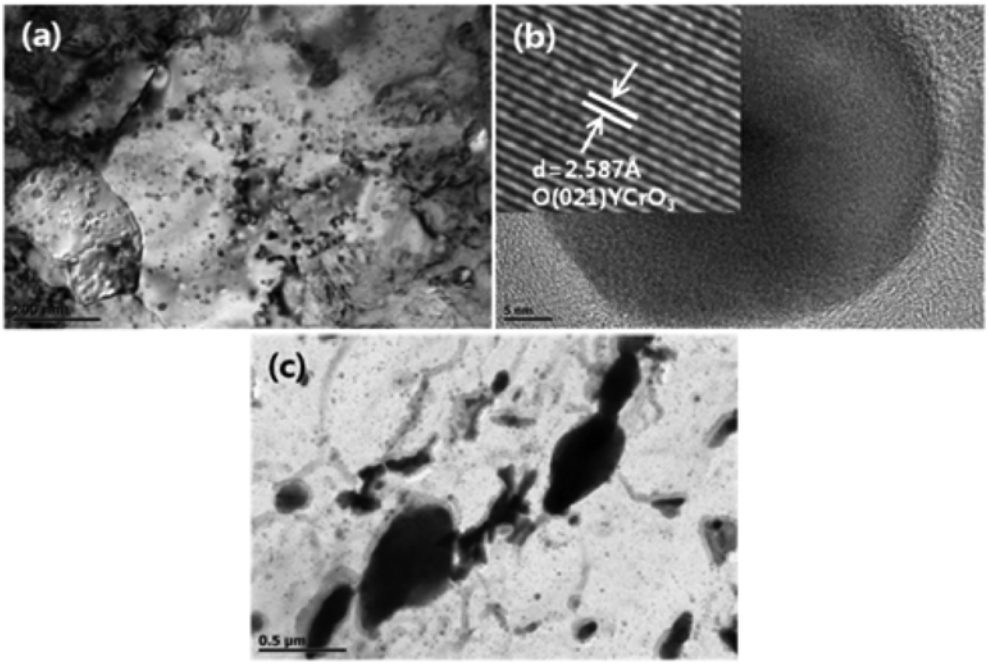

Fig. 5. TEM images of Fe-based ODS alloy after sintering at 1100°C: (a) Specimen sintered by using MA90, (b) HREM image of $YCrO_3$ obtained by the replica method, specimen sintered by using MA90, and (c) specimen sintered by using MA10.

References

[1] M. Brocq, B. Radiguet, J.-M. Le Breton, F. Cuvilly, P. Pareige and F. Legendra: Acta Meter., **58** (2010) 1806-1814.

[2] M. Klimiankou, R. Lindau and A. MÖslang: J. Cryst. Growth, **249** (2003) 381-387.

[3] H. Sakasegawa, L. Chaffron, F. Legendre, L. Boulanger, T. Cozzika, M. Brocq and Y. de Carlen: J. Nucl. Mater., **394** (2009) 115-118.

[4] S. Ukai, S. Mizuta, T. Yoshitake, T. Okuda, M. Fujiwara, S. Hagi and T. Kobayashi: J. Nucl. Mater., **283-287** (2000) 702-706.

[5] Z. Okasiuta and N. Baluc: J. Nucl. Mater., **374** (2008) 178-184.

[6] M. Alinger, G. Odette and D. Hoelzer: J. Nucl. Mater., **329-333** (2004) 382-386.

[7] M. Yamamoto, S. Ukai, S. Hayashi, T. Kaito and S. Ohtsuka: "Formation of residual ferrite in 9Cr-ODS ferritic steels" Meter. Sci. Engin., **527** (2010) 4418-4423.

[8] S. M. Hong, J. J. Park, E. K. Park, M. K. Lee, C. K. Rhee, J. M. Kim and J. K. Lee: J. Kor. Powd. Met. Ins., **19** (2012) 219.

[9] M. Klimiankou, R. Lindau and A. MÖslang: J. Nucl. Mater., **329-333** (2004) 347-351.

[10] G. Pintsuk, Z. Oksiuta, J. Linke and N. Baluc: J. Nucl. Mater., **396** (2010) 20-25.

[11] J. G. Lee, S. M. Hong, J. J. Park, M. K. Lee, S. J. Hong and C. K. Rhee: Mater. Charact., **61** (2010) 1290-1293.

[12] V. de Castro, T. Leguey, A. Muňoz, M.A. Monge, R. Pareja, P. Fernández, A. M. Lanoha: J. Nucl. Mater., **386-388** (2009) 449-452.

[13] G. Yu, N. Nita and N. Baluc: Fusion. Engin. Design., **75-79** (2005) 1037-1041.

[14] B. N. Goshchitskii, V. V. Sagaradze, V. I. Shalaev, V. L. Arbuzov, Y. Tian, W. Qun and S. Jiguang: J. Nucl. Mater., **307-311** (2002) 783-787.

[15] Z. Oksiuta and N. Baluc: Nucl. Fusion., **49** (2009) 9.